The 19th Conference of Mechanical Engineering Network of Thailand
19-21 October 2005, Phuket, Thailand

Characteristics of Temperature Distribution in Swirling Jets in Counterflow

P. Uppathamnarakorn[1], W. Wangjiraniran[2], A. Pimpin[1*], and A. Bunyajitradulya[1]

Department of Mechanical Engineering[1]
Department of Nuclear Technology[2]
Faculty of Engineering, Chulalongkorn University, Bangkok 10330, Thailand
* Email: alongkorn.pimpin@gmail.com

Abstract

Effects of swirl on the characteristics of temperature distribution of a heated swirling jet in counterflow are investigated. Temperature distributions in the cross planes downstream of the jet are surveyed. The experiments are conducted at a fixed effective velocity ratio *r* of 4.6, swirl ratios (*Sr*) of zero (no swirl), 0.11, 0.22, and 0.33, and a Reynolds number of 10,000. The results show that swirl promotes jet spreading and temperature decay as well as shortens potential core and penetration depth, signifying enhancement in large-scale mixing. In addition, the results also show that the mean temperature distributions in the cross planes downstream of the jets, both without and with swirl, are fairly axisymmetric. This suggests (within the current experiment limit) that, albeit the highly unstable and unsteady instantaneous flow, both jets in counterflow - without and with swirl - have no preferred azimuthal direction and no preferred azimuthally asymmetric mode.

Keywords: Jet in counterflow, swirling jet, temperature distribution, mixing enhancement, penetration depth.

1. Introduction

Jet flows in a moving stream are flows of many technological applications. They can be found in vast areas such as energy and combustion, propulsion, heat transfer, and environment. One of the flows in this class of flow configuration is a jet in counterflow, which is often found in environment where river or wasted water is discharged into the sea. In such case, the characteristics of the jet govern the dispersion and deposition of pollutants and the distribution of temperature, which may affect the ecosystem and the environment in that area. On the other hand, because of its flow reversal and enhanced dilution/mixing characteristics, in comparison with jets in co- and crossflow, the potential areas of application of a jet in counterflow therefore include combustion and mixing processes. However, these practical uses are still hindered by the complexity and the instability of the flow itself as well as our relatively little knowledge of the flow and how to manipulate and control the flow, [1].

Briefly, the features of a jet in counterflow are as follows. As a jet is issued into a counterflow, it penetrates deep into the counterflow for some axial distance x_p, called *penetration depth*, and spreads laterally for some radial distance before it is deflected backward by the counterflow, [1],[2],[4],[5]. Depending upon the jet-to-counterflow velocity ratio $r = u_j / u_{cf}$, where u_j is the axial velocity of the jet at the jet exit and u_{cf} is the velocity of the uniform counterflow, the jet may be '*stable*' or '*unstable*', [2], [3], [6]. At low velocity ratio ($r < 1.3-1.4$), the jet is stable, symmetric, with nearly constant downstream extent and regular vortex shedding. At intermediate velocity ratio just above 1.3-1.4, the onset of the unstable flow sets in and the unstable flow coexists with the stable flow, with the two alternating in time. In addition, at the velocity ratio below 3.0, the flow is quite sensitive to directional perturbation. At high velocity ratio ($r > 3.4$), the jet is virtually unstable, with fluctuations in both axial and radial extents. In addition, the flow field can be divided into two regions: the near field and the far field. In the near field, where the velocity of the jet is still high, the jet flow is dominant and the behavior of the jet is much like that of a jet issued into a stagnant ambient. In the far field, as the velocity further decays, the counterflow is dominant. The tip of the jet interacts with the counterflow, deflects and oscillates with a low frequency in an unstable manner, and the jet is convected backwards. Due to these deflection and oscillation, the instantaneous flow field is highly unsteady and asymmetric. On the contrary, the mean flow shows good symmetry.

Although previous studies have shed some lights on the characteristics of a jet in counterflow in various flow regimes, fewer studies have addressed the issue of modified flow configuration in order to pave the way for further flow manipulation and control. In this present study, we have explored the effects of swirl on the characteristics of temperature distribution of a heated jet in counterflow, the results of which are indicative of its effects on large-scale mixing.

2. Experimental Setup and Conditions

Figure 1 shows the configuration of a swirling jet in counterflow being investigated in this work. The experimental setup consists of two main components: a wind tunnel and a rotating-pipe jet setup. The wind tunnel, which is used to generate uniform counterflow, is

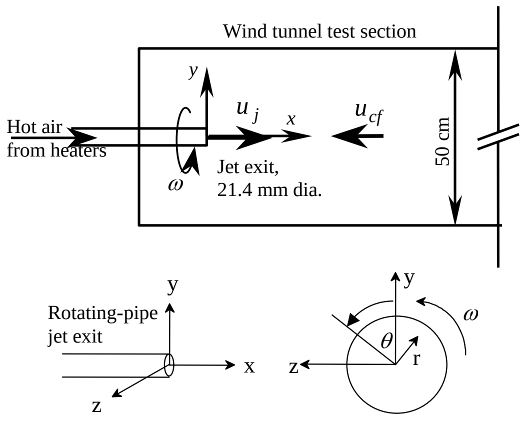

Fig. 1. Swirling jet in counterflow configuration and coordinate system.

a wide-angle screened-diffuser blower type with the test section of 0.5x0.5 m^2 in cross section and 2.4 m in length. At the end of the test section, the rotating-pipe jet setup which is used to generate a swirling jet is installed.

In order to generate a heated swirling jet, air from a blower is passed through a heating chamber, installed with one 0.5-kw and two 2-kw electric heaters. After the heaters, hot air is passed through three perforated plates, serially installed in order to promote mixing and making the exit flow uniform in temperature. Hot air is then passed through the rotating pipe with honeycomb section.

The rotating pipe, driven by a 2-hp motor with frequency inverter, consists of 3 stainless steel pipe sections, connected to one another by collars. The pipes in these sections are 21.4 mm in inner diameter (*d*) and 2 mm in thickness. The three sections are 14*d*, 19*d*, and 54*d*, in length respectively from upstream to downstream. The first section is an empty pipe. In the second section, a honeycomb is installed in order to impart swirl to the incoming air stream. The honeycomb is made from small brass tubes of 2.2 mm in inner diameter, 0.5 mm in thickness, and the section length in length, packed inside the section. Each end of the honeycomb is covered by a 30×35 (mesh$\times$SWG) screen. The third section before the jet exit is empty and without flow conditioning device. Using the rotating-pipe with honeycomb, the resulting swirling jet has non-zero tangential velocity and non-zero circulation.

Measurements

Initial conditions for velocity and temperature of the jet are measured at the jet exit plane ($x/d=0$) and along the *y*-traverse while the counterflow is turned *on*. The coordinate system employed in this experiment is shown in Fig. 2. Initial velocity profile for the case without swirl is measured with a pitot probe, while those with swirl, with both axial (*u*) and tangential (*w*) velocity components, are measured with a three-tube cobra-type yaw probe, [7]. The probe is made from three hypodermic needles, having outer diameter of 0.5 mm and inner diameter of 0.32 mm. Initial temperature profiles are measured with type-K thermocouple probe, while the temperature distributions in the cross planes are measured with type-T thermocouple probe.

Experimental and Initial Conditions

Experiments are conducted at the counterflow velocity (u_{cf}) of 2.0 ± 0.1 m/s, the area-averaged jet axial velocity ($\bar{u}_j$) of 9.9 ± 0.4 m/s, the counterflow temperature (T_{cf}) of 30.3 ± 0.9 ^{o}C, and the area-averaged jet temperature ($\bar{T}_j$) of 76.8 ± 3.1 ^{o}C. These result in the effective jet-to-counterflow velocity ratio (*r*) of 4.6. Note that due to the difference in jet and counterflow temperatures, the effective jet-to-counterflow velocity ratio in this experiment is defined as $r=\sqrt{\rho_j \bar{u}_j^2/\rho_{cf} u_{cf}^2}$, where ρ_j is the jet air density calculated from the area-averaged jet exit temperature and ρ_{cf} is the counterflow air density. Other flow conditions are as follows: the jet Reynolds number of 10,000; the density ratio ρ_j/ρ_{cf} of 0.87; the densimetric Froude number (*Fr*), defined as $Fr=\sqrt{(\rho_{cf}-\rho_j)gd/\rho_{cf}u_{cf}^2}$, of 0.08; and Fr/r, which results in $Fr/r=\sqrt{(\rho_{cf}-\rho_j)gd/\rho_j\bar{u}_j^2}$, of 0.02. The effects of swirl are investigated by varying the swirl ratio (*Sr*), defined as $Sr=(\omega R)/\bar{u}_j=w_p/\bar{u}_j$, where ω is the angular velocity of the rotating pipe, R is the pipe inner radius, and w_p is the peripheral inner pipe wall speed, from zero (no swirl), 0.11, 0.22, to 0.33.

Figure 2 shows the initial profiles of the normalized axial velocity $u/u_{\max}$, where $u_{\max}$ is the maximum axial velocity along the traverse which practically positions at the center of the jet. The results show that all profiles are fairly similar and symmetric, and they are in good agreement with 1/7 power law of the turbulent profile. Nonetheless, it is observed that near the pipe wall, the velocities of the swirling cases are consistently slightly lower than that of the non-swirling case.

Figure 3 shows the initial profiles of the normalized tangential velocity (w/w_p) together with the parabolic profile, see e.g., [8]. The results show some deviation from the parabolic profile at low swirl ratio. Namely, the case with lower swirl shows some lagging from the parabolic profile. However, the deviation decreases as swirl ratio increases. At the highest swirl of 0.33, the profile is in good agreement with the parabolic profile.

In this respect, the deviation deserves some discussion. Specifically, it is considered to be due to the difference in the dimensionless flow-developing length based on a pitch length scale $l_p=l_x/p$, where l_x is the flow-developing distance measured from the honeycomb exit and *p* is the pitch length scale. The pitch length scale is defined as the axial distance

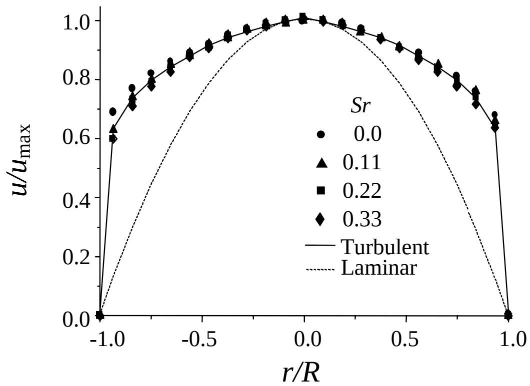

Fig 2. Initial axial velocity profiles of the jets.

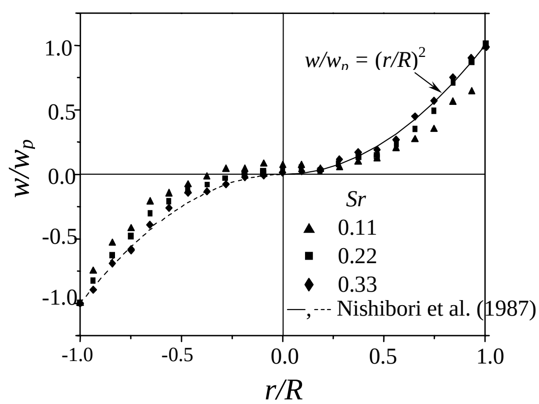

Fig 3. Initial tangential velocity profiles of the jets.

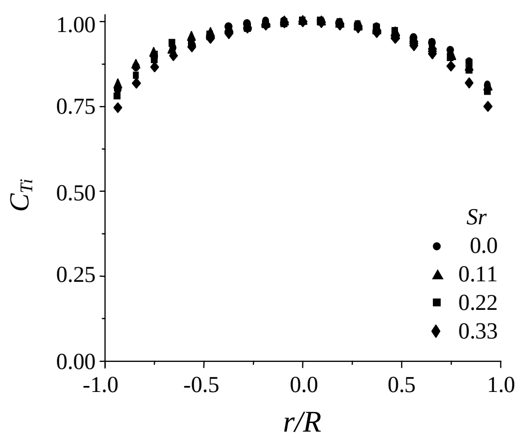

Fig 4. Initial temperature profiles of the

corresponding to one revolution of the azimuthal flow, $p = \pi d / Sr$; thus, $l_p = Sr(l_x / d) / \pi$. In this regard, due to a fixed third section length (54*d*) after the honeycomb, the flows with swirl of 0.11, 0.22, and 0.33 will have developed by different distances of l_p = 1.9, 3.8, and 5.6, respectively, before they reach the pipe exit. With the currently limited data, the current results nonetheless suggest that, in order to reach a parabolic profile, the required development length can be in the order of l_p = 5 or more, at least near this range of Reynolds number.

In presenting the results on temperature in this study, various temperature coefficients will be used depending upon the appropriate reference temperature T_{ref} chosen. These dimensionless temperature coefficients C_T are generically defined as

$$C_T = (T - T_a)/(T_{ref} - T_a) ,$$

where T is the local measured temperature, and T_a is the ambient temperature, which is always equal to the temperature of the counterflow T_{cf} in this experiment since the measurements are always made when the counterflow is turned on. Note that C_T indicates the fraction of the local excess temperature from the ambient, $(T - T_a)$, to that of the reference temperature $(T_{ref} - T_a)$.

Figure 4 shows the initial profiles of the normalized temperature C_{Ti} , in which $T_{ref} = T_{\max}$ is the maximum temperature along the radial traverse. The results show fairly similar profiles near the center and increasing deviation towards the pipe wall, with the flow with higher swirl exhibiting lower temperature towards the wall.

3. Results and Discussions

Temperature Distributions

Temperature distributions in the cross planes downstream of the jet for cases *Sr* = 0 and *Sr* = 0.33 are shown in Fig. 5. (The results for cases *Sr* = 0.11 and 0.22, though not shown here, show similar characteristics.) The results are presented in terms of C_{TG} , in which $T_{ref} = \overline{T}_j$ is the area-averaged temperature of the jet at the jet exit. The uncertainty in C_{TG} is estimated to be 0.05, while the resolution of the contour in these figures is 0.1. The subplots at *x/d* = 16 in case *Sr* = 0 and at *x/d* = 14 and 16 in case *Sr* = 0.33 are intentionally left empty to indicate that at these stations the normalized temperature has already decayed to lower than 0.1. For both cases, the results show initial growth and later collapse in jet extent along the downstream direction (with respect to the jet initial velocity). In addition, they also show fairly axisymmetric temperature distributions for this mean temperature measurement. Note that for the instantaneous flow, however, the flows are expected to be highly unsteady and asymmetric. The result then suggests that, at least within the current experiment limit, both flows – without and with swirl – have no preferred azimuthal direction and no preferred azimuthally asymmetric mode. When the two flows are compared,

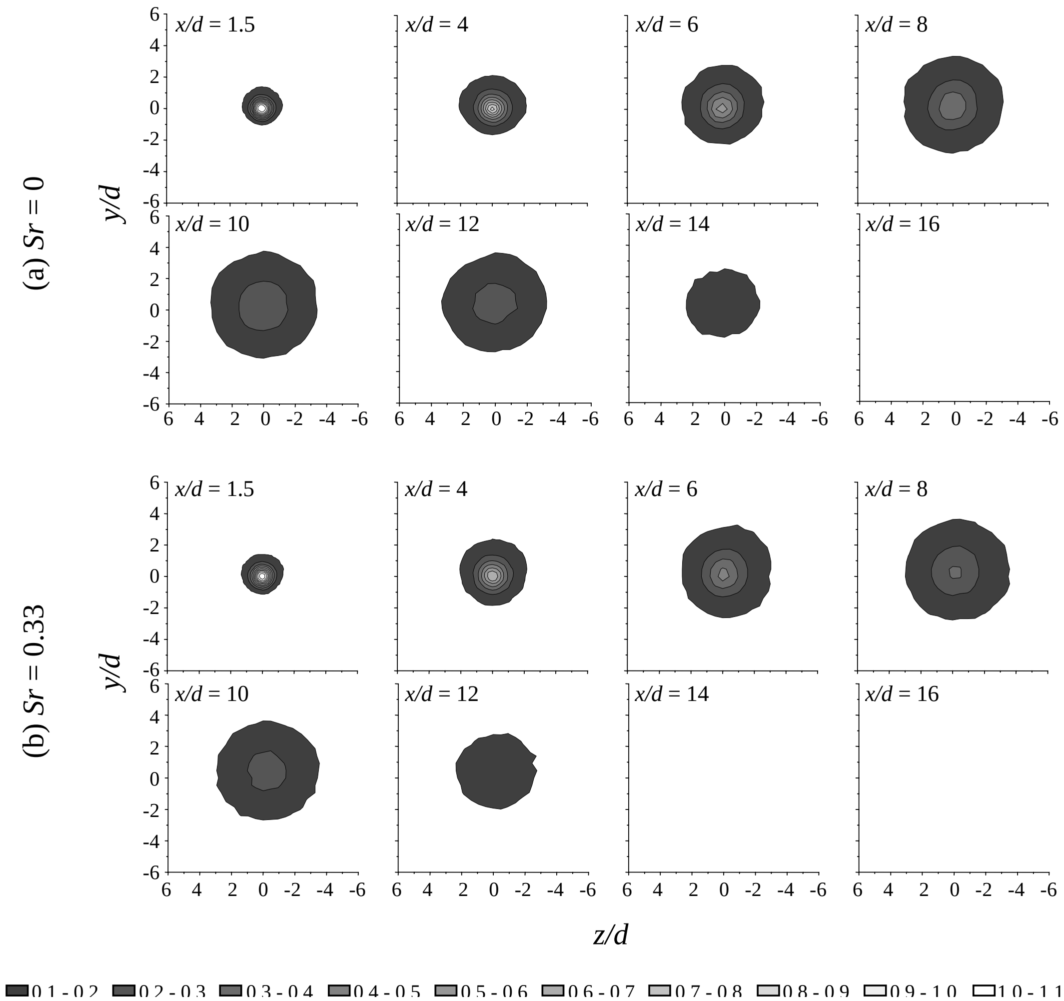

Fig. 5. Temperature distribution in the cross planes, C_{TG}: (a) *Sr* = 0 (no swirl), (b) *Sr* = 0.33. Note that the empty subplots at *x/d* = 16 in case *Sr* = 0 and *x/d* = 14 and 16 in case *Sr* = 0.33 are intentional to indicate that at these stations, the normalized temperature decays to less than 10% of the initial excess temperature.

the results show that the temperature for the case with swirl *Sr* = 0.33 decays faster than that for the case without swirl. Specifically, the temperature decays to within 10% of the initial excess temperature at the distance of *x/d* = 12 and 14 for the case with and without swirl, respectively.

In order to investigate the characteristics of these jets in more details, three global characteristics, namely, centerline temperature decay, penetration depth, and jet spreading, are investigated as follows.

Centerline Temperature Decay

The centerline temperature decays, expressed in terms of $C_{T_{CL}}$ in which $T_{ref} = T_{j,c}$ is the temperature at the jet center at the jet exit, are shown in Fig. 6(a). The results indicate that centerline temperatures of the swirling jets decay faster than that of the jet without swirl; the higher the swirl, the faster the decay. Specifically, when swirl ratio is increased from zero to 0.33, the fifty-percent decay length, the length at which the excess temperature decreases to half of the original value at the jet exit, is shortened from 6*d* to 5*d*, approximately 17%. A closer look at the near field in Fig. 6(b) also shows that most of the reduction manifests in the reduction in the potential core. This indicates that the mechanism that enhances entrainment and large-scale mixing is focused in the near filed near the jet exit.

Penetration Depth

In order to further characterize the characteristics of the swirling jet in counterflow, the penetration depth of the jet is investigated. In this respect, the following scheme is used to identify and characterize the penetration depth.

Chan and Lam [9], worked in the Lagrangian frame, gave the centerline velocity decay for a plain jet in

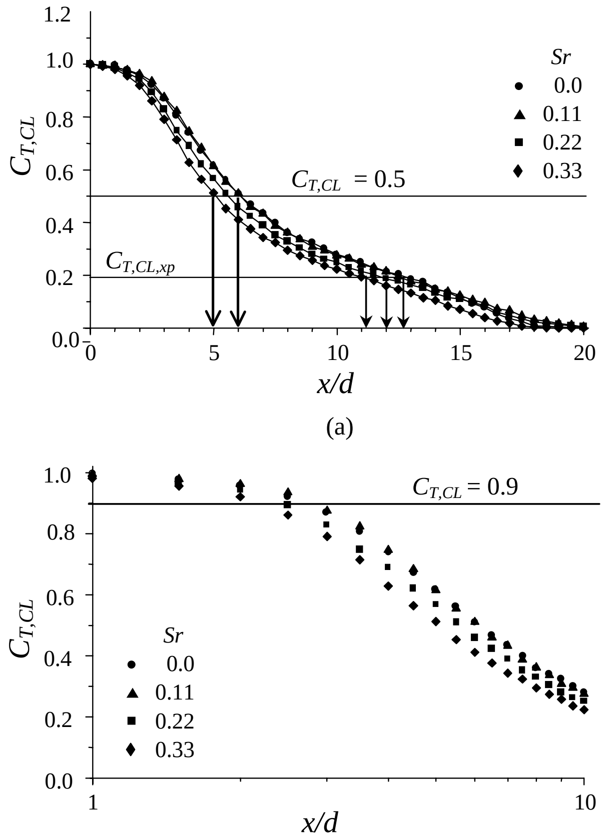

(a)

(b)

Fig. 6. Centerline temperature decay: (a) overall view, illustrated also are the fifty-percent decay lengths for Sr = 0 and Sr = 0.33 (two arrows down) and the scheme for locating the penetration depth at $C_{T,CL,xp}$ (three arrows down); (b) a closer look at the near field, the line $C_{T,CL}$ = 0.9 is for ease of viewing.

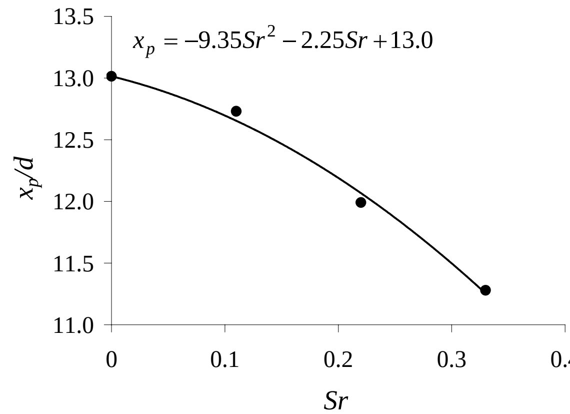

Fig. 7. Penetration depth as a function of swirl ratio.

counterflow (without swirl). By defining the (*velocity-based*) *penetration depth* x_p as the distance at which the centerline velocity decays to zero, they calculated the penetration depth from the centerline velocity decay relation and found good agreement with experimental data. In order to apply their result to ours, two issues arise. Firstly, their definition of penetration depth is based on velocity field, hence it cannot be applied to our results on temperature field directly. Secondly, in their study the effect of swirl was not investigated and therefore was not included.

As a result, in order to identify the penetration depth from temperature field in our case of the jets in counterflow with swirl, the following scheme is applied. If their model is applied to the current case of the jet without swirl (Sr = 0) with the effective velocity $r = 4.6$, the penetration depth is found to be $x_p / d = 13.0$. At this distance, the centerline temperature coefficient for this case is found to be $C_{T,CL} = 0.19$. This value of normalized temperature, denoted by $C_{T,CL,xp}$, is then adopted as also indicative of the penetration depth for the cases with swirl. The penetration depths for cases Sr = 0.11, 0.22, and 0.33, are then found to be 12.7d, 12.0d, and 11.3d, respectively, Fig. 6(a). Figure 7 shows the relation between the penetration depth and the swirl ratio as derived from this scheme. It indicates that the penetration depth gradually decreases as swirl ratio increases. From these results, a simple parabolic function is fitted with the constraint: $\left(x_p / d\right)_{Sr=0} = 13.0$, and the result is $\left(x_p / d\right) = -9.35Sr^2 - 2.25Sr + 13.0$. Note that this correlation is derived from $Sr \le 0.33$ at $r = 4.6$ only. Nonetheless, a general simple correlation for other velocity and swirl ratios in this neighborhood ranges is postulated to be in similar form: $(x_p / d) = aSr^2 + bSr + (x_p / d)_{Sr=0}$, where $(x_p / d)_{Sr=0}$ is the penetration depth of a plain non-swirling jet in counterflow at the effective jet-to-counterflow velocity ratio r, and a and b can be constants or functions of r. Note that the penetration depth given here is a minor revision from that of Uppathamnarakorn [10]. The revision is for the more exact determination of the penetration depth from Chan and Lam's model.

Finally, it should be noted that, albeit the above scheme is initially introduced by basing on the correspondence to the velocity field, the derived penetration depth however can be independently considered as a *temperature-field penetration depth*. That is, it is the distance at which the normalized centerline temperature decays to $C_{T,CL,xp}$.

Jet Spreading: Equivalent Radius

In order to investigate the spreading of the jets, the equivalent radius of the jets is calculated. The equivalent radius at α, R_α, is defined as the radius of a circle whose area is equal to the cross section area of the jet in which $C_{TL} \ge \alpha$. Note that C_{TL} is defined with

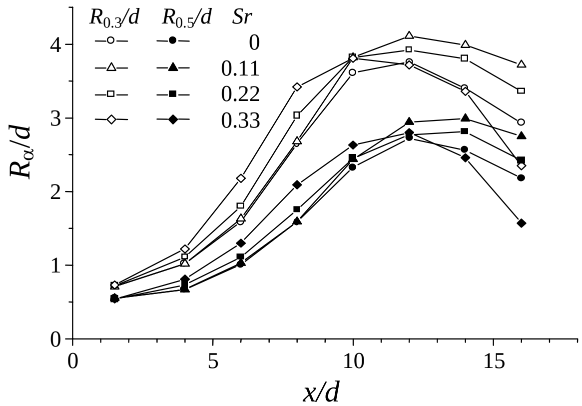

Fig. 8. Equivalent radii of the jets.

$T_{ref} = T_{C\,\max}$, where $T_{C\,\max}$ is the maximum temperature at the local cross section. Figure 8 shows the results for the equivalent radii at α = 0.5 and 0.3, $R_{0.5}$ and $R_{0.3}$, respectively. The results indicate that swirl enhances the jet spreading; the larger the swirl, the larger the spreading.

In summary, these characteristics of swirling jets in counterflow point to the effects of swirl in promoting entrainment and large-scale mixing of the jet in counterflow, at least within the limit of the current parameters. In addition, as indicated by the reduction in the potential core, the mechanism for mixing enhancement is likely to be due to the modification of the flow structure near the jet exit. Hence, better understanding of the flow structure in this region may shed some light on the physical mechanism as well as may give useful information on the manipulation of the flow.

4. Conclusions

The effects of swirl on temperature distribution in heated swirling jets in counterflow are investigated. The results show that swirl promotes faster jet spreading and temperature decay as well as reductions in potential core and penetration depth. When swirl ratio is increased from zero to 0.33, the fifty-percent centerline decay length is shortened by 17% from that of the jet without swirl. The present study also incorporates the effect of swirl on the penetration depth of a jet in counterflow and gives the result as a simple parabolic correlation.

Furthermore, the results also show fairly axisymmetric mean temperature distributions in the cross planes downstream of the jet for both jets without and with swirl. This suggests (within the current experiment limit) that, albeit the highly unstable and unsteady instantaneous flow, both jets in counterflow - without and with swirl - have no preferred azimuthal direction and no preferred azimuthally asymmetric mode.

Acknowledgement

Graduate Research Fund Year 2000 from The National Energy Policy Office (NEPO), Graduate Student Research Grant from Chulalongkorn University's Graduate School, and Faculty of Engineering Research Fund No. 163-ME-2543 are gratefully acknowledged.

References

[1] S. Beltaos and N. Rajaratnam, "Circular turbulent jet in an opposing infinite stream," in *Proc. 1st Can. Hydraul. Conf.*, Edmonton, 1973, pp. 220-237.

[2] M. Yoda and H. E. Fiedler, "The round jet in a uniform counterflow: flow visualization and mean concentration measurements," *Exp. Fluids*, Vol. 21, 1996, pp. 427-436.

[3] S. Bernero and H. E. Fiedler, "Application of particle image velocimetry and proper orthogonal decomposition to the study of a jet in a counterflow," *Exp. Fluids* [Suppl.], Vol. 29, 2000, pp. S274-S281.

[4] D. F. Hopkins and J. M. Robertson, "Two-dimensional incompressible fluid jet penetration," *J. Fluid Mech*., Vol. 29, 1967, pp. 273-287.

[5] O. König and H. E. Fiedler, "The structure of round turbulent jets in counterflow: a flow visualization study," in Advances in Turbulence III, Springer, 1991, pp. 61-66.

[6] S. Bernero, "A turbulent jet in counterflow," Ph.D. thesis, Technical University of Berlin, Germany, 2000.

[7] S. H. Chue, "Pressure probes for fluid measurement," *Prog. Aero. Sci*., Vol. 16, No.2, 1975, pp. 147-223.

[8] K. Nishibori, K. Kikuyama, and M. Murakami, "Laminarization of turbulent flow in the inlet region of an axially rotating pipe," *Bull. JSME*, Vol.30, No. 260, 1987, pp. 255-262.

[9] H. C. Chan and K. M. Lam, "Centerline velocity decay of a circular jet in a counterflowing stream," *Phys. Fluids*, Vol. 10, No. 3, 1998, pp. 637-644.

[10] P. Uppathamnarakorn, "Effects of the swirl number on mixing characteristics of a heated swirling jet in counterflow," M.S. Thesis, Department of Mechanical Engineering, Faculty of Engineering, Chulalongkorn University, Thailand, 2001.